Portugaliae Electrochimica Acta 2010, 28(5), 321-335

DOI: 10.4152/pea.201005321

PORTUGALIAE ELECTROCHIMICA ACTA
ISSN 1647-1571

Inhibitive Performance of Gemini Surfactants as Corrosion Inhibitors for Mild Steel in Formic Acid

Farhat A. Ansari,[*] M. A. Quraishi

Department of Applied Chemistry, Institute of Technology
Banaras Hindu University, Varanasi 221 005, India

Received 07 October 2009; accepted 12 November 2010

Abstract

Three new gemini surfactants referred to as n-2-n (where n= 6, 12, 16) were developed as corrosion inhibitors for mild steel. Their critical micelle concentration (cmc) at equilibrium in water at 30^{o}C was determined. Corrosion inhibition studies of mild steel in formic acid by gemini surfactants were conducted by using weight loss, electrochemical polarisation and electrochemical impedance spectroscopy (EIS) measurements. Scanning electron microscopic study (SEM) was also used to investigate the surface morphology of inhibited and uninhibited metal samples. The results obtained show that the surfactants studied are good mixed type inhibitors. The result was also correlated with several factors, including the chain length of the hydrophobic chains, critical micelle concentration (cmc) and adsorption free energy of these inhibitors. The adsorption of all the gemini surfactants was found to follow Langmuir adsorption isotherm. EIS results indicate that the change in the impedance parameters (R_t and C_{dl}) with concentration of inhibitors was due to the formation of a protective layer on the surface of mild steel.

Keywords: gemini surfactants, mild steel, electrochemical techniques, scanning electron microscopy.

Introduction

Organic acids constitute a group of the most important chemicals currently in use in industry. They are widely used in the chemical industries for preparation of various chemicals, drugs, plastics and fibers. Few corrosion studies of metals in organic acids have been made [1–3]. However organic acids are weak acids, but provide sufficient protons to act as true acids toward most metals [4]. Organic

[*] Corresponding author. E-mail address: farhataisha@gmail.com

acid strength tends to increase as molecular weight decreases. Low molecular weight acids such as formic acid are quite corrosive relative to longer chain acids. Corrosion inhibition studies of metals in organic acids are scarce in comparison with similar studies in mineral acids [5-7]. The application of surface–active agents containing nitrogen, sulphur, or both give excellent corrosion inhibition for carbon steel alloys in acidic medium [8, 9]. It was found that these substances have remarkable inhibition efficiency near their critical micellar concentration (cmc) values. Recently, a new generation of surfactants, gemini surfactants, has aroused great concerns. This kind of surfactant contains two hydrophilic groups and two hydrophobic groups in the molecule, separated by a rigid or flexible spacer, rather than one hydrophilic group and one hydrophobic group for conventional surfactants, and they are more efficient at reducing surface tension and forming micelles than conventional surfactants.

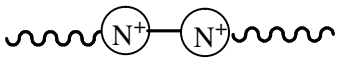

Gemini surfactants show many unique properties as compared with single chain conventional surfactants, such as lower cmc(s), better wetting properties and more effectiveness in lowering the surface tension of water [10-12].
In this study, three gemini surfactants, N-hexane-diyl-1,2-ethane-bis ammonium bromide (HEAB), N-dodecane-diyl-1,2-ethane-bis ammonium bromide (DDEAB), N-hexadecane-diyl-1,2-ethane-bis ammonium bromide (HDEAB), were developed as novel corrosion inhibitors for mild steel in 20% formic acid. Their inhibition effectiveness was evaluated by electrochemical studies, and surface adsorption phenomena were investigated by scanning electron microscopy.

Table1. Name and molecular structure of the gemini surfactants.

S. No	Molecular structure	Name and abbreviation
1.	$CH_3\text{-}(CH_2)_5\text{-}\overset{\overset{H}{|}}{\underset{\underset{H}{|}}{N}}{}^{+}\text{-}CH_2\text{-}CH_2\text{-}\overset{\overset{H}{|}}{\underset{\underset{H}{|}}{N}}{}^{+}\text{-}(CH_2)_5\text{-}CH_3 \quad 2Br^-$	N-hexane-diyl-1,2-ethane bis ammonium bromide (HEAB)
2.	$CH_3\text{-}(CH_2)_{11}\text{-}\overset{\overset{H}{|}}{\underset{\underset{H}{|}}{N}}{}^{+}\text{-}CH_2\text{-}CH_2\text{-}\overset{\overset{H}{|}}{\underset{\underset{H}{|}}{N}}{}^{+}\text{-}(CH_2)_{11}\text{-}CH_3 \quad 2Br^-$	N-dodecane-diyl-1,2-ethane bis ammonium bromide (DDEAB)
3.	$CH_3\text{-}(CH_2)_{15}\text{-}\overset{\overset{H}{|}}{\underset{\underset{H}{|}}{N}}{}^{+}\text{-}CH_2\text{-}CH_2\text{-}\overset{\overset{H}{|}}{\underset{\underset{H}{|}}{N}}{}^{+}\text{-}(CH_2)_{15}\text{-}CH_3 \quad 2Br^-$	N-hexadecane-diyl-1,2-ethane bis ammonium bromide (HDEAB)

Experimental

Material preparation

AR grade formic (MERCK) and doubled distilled water were used for preparing test solutions of 20% formic acid for all studies. The gemini surfactants were synthesized following a procedure as described earlier [10]. The compounds were characterized through their spectral data; their purity was confirmed by thin layer chromatography (TLC) and by infrared spectroscopy. Names and molecular structures of the synthesized compounds are given in Table 1.

Surface tension studies

The surface tension measurements of all the three synthesized gemini surfactants were made at 30±2 ^{o}C using Du Nuoy ring method at 30±1 ^{o}C with a digital tensiometer (model K 10ST; Kruss).

Weight loss measurement

Mild steel strips having composition (C 0.14%, Mn 0.035%, Si 0.17%, S 0.025%, P 0.03 % and balance Fe) were used for the experiments. The mild steel plate of size (2.0 x 2.5 x 0.025 cm) was used for weight loss measurements. Weight loss study was carried out at 30-60 ^{o}C temperature and 24 h time duration in 20% formic acid solution. All the concentrations of the inhibitor taken for weight loss, were taken in ppm by weight. The experiments were performed as per ASTM method described [13]. Corrosion rate and inhibition efficiency (%) were calculated by following two equations:

$$CR = \frac{K \times W(mg)}{T(h) \times A(cm^2) \times D(g/cm^3)} \quad (1)$$

where CR - corrosion rate; K- constant; W - mass loss [mg]; T- corrosion period [h]; A- specimen area [cm^2]; D- density [g/cm^3], and

$$IE = \frac{CR^O - CR'}{CR^O} \times 100 \quad (2)$$

where, CR^o - corrosion rate without inhibitor; CR' - corrosion rate with inhibitor; IE- inhibition efficiency.

Electrochemical studies

The equivalent circuit model employed for this system is shown below:

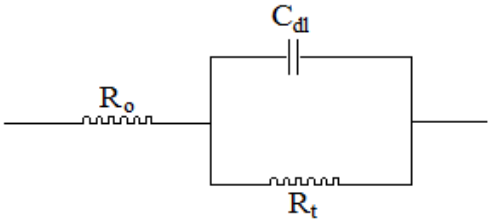

R is a resistor (R_o= solution resistance and R_t = charge transfer resistance), and C_{dl} represents the double layer capacitance.

All electrochemical measurements were performed using a conventional three electrode cell assembly at 30±1 ^{o}C [14, 15], consisting of a saturated calomel

electrode (SCE), the mild steel coupon and a rectangular platinum foil as reference, working and counter electrodes, respectively. Mild steel, strips of the above composition, coated with commercially available lacquer with an exposed area of 1.0 cm^2 were used and the experiments were carried out at temperature (30 ± 1 ^oC). The polarization and impedance measurements were carried out using a Gamry Potentiostat / Galvanostat (model 300) with EIS software, Gamry-Instruments Inc., USA. Tafel polarization was carried out from cathodic potential of - 0.25 V vs. open corrosion potential (OCP) to an anodic potential of +0.25 V vs. OCP at a sweep rate 1 mV/sec to study the effect of the inhibitor on corrosion of mild steel. The corrosion inhibition efficiency (IE) was evaluated from I_{corr} values using the relation:

$$IE = \frac{I^o corr - I^i corr}{I^o corr} \times 100 \quad (3)$$

where $I^o corr$ - corrosion current density in absence of the inhibitor; $I^i corr$- corrosion current density in presence of the inhibitor

The impedance measurements were done in frequency range 100 kHz to 10 mHz with 10 points per decade at OCP after a stabilization period of 30 min. A 10 mV sine wave ac voltage was used to perturb. The potential values reported here were versus SCE. The charge transfer resistance values were obtained from the diameter of the semi circles of the Nyquist plots. The inhibition efficiency of the inhibitor was calculated from the charge transfer resistance values using the following equation:

$$IE = \frac{(1/R^o{}_t) - (1/R^i{}_t)}{(1/R^o{}_t)} \times 100 \quad (4)$$

where: R^o_t - charge transfer resistance in absence of the inhibitor (ohmcm^2); R^i_t - charge transfer resistance in presence of the inhibitor (ohmcm^2).

The interfacial double layer capacitance (C_{dl}) values have been estimated from the impedance value by the equation:

$$C_{dl} = \frac{1}{2\pi R_t f} \quad (5)$$

R_t - charge transfer resistance; f - frequency (Hz).

Scanning electron microscopy

The scanning electron microscope (SEM) images of corroded surface of some samples in the absence and presence of the inhibitor were taken using a SEM model No. 435 VP LEO. The specimens were thoroughly washed with double distilled water before examination. The photographs have been taken from that portion of specimen from where better information was obtained. They were photographed at appropriate magnifications (2500-3000 micrometer). To understand the morphology of the steel surface in absence and presence of the inhibitors, three samples have been examined:

i) polished mild steel specimen;

ii) mild steel specimen dipped in 20% formic acid for 24 hours;
iii) mild steel specimen dipped in 20% formic acid containing 300-ppm HDEAB for 24 hours.

Results and discussion

Surface tension measurement

The critical micelle concentration (cmc) values of the synthesized gemini surfactant were determined from the break point of the surface tension (m Nm^{-1}) versus concentration (ppm) curves shown in Fig. 1. The behaviour of the gemini surfactants was explained from their surface tension values. The lower surface tension values correspond to higher surfactant adsorption at the interface. This is due to the fact that the presence of the surfactant molecule at the interface disturbs the interfacial force of the water surface and breaks down the hydrogen bonds that have been formed. Thus the surface tension decreases.

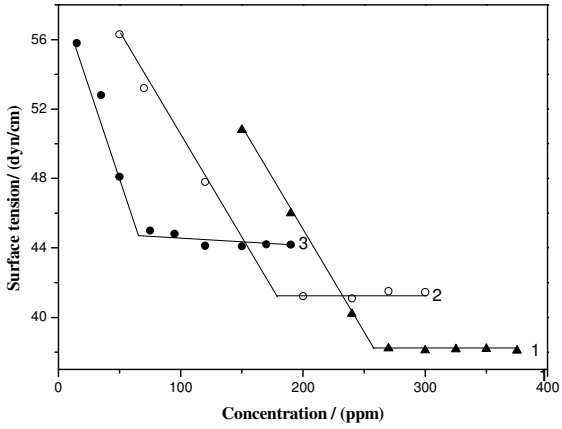

Figure 1. Surface tension measurement of gemini surfactants studied at 30 ± 2 ^{o}C (1-HEAB, 2- DDEAB, 3- HDEAB).

Weight loss measurement

The values of percentage inhibition efficiency (%IE) and corrosion rate (CR) obtained from weight loss method at different concentrations at 30 ºC are summarized in Table 2. It is observed from Fig. 2(a) that the inhibition efficiency of all the gemini surfactants increases with increasing the inhibitor concentration in formic acid and shows a sharp increase in the inhibition efficiency around their cmc (s) values, and further increase in the inhibitor concentration does not show any appreciable change in the inhibition efficiency. Critical micellar concentration (cmc) is the concentration where surfactants in solution change their initial molecular solvated state.

The values of IE are in the order HDEAB > DDEAB > HEAB. The alkyl chain length and the structure play an important role in the inhibition efficiency of the synthesized gemini surfactants. The geometrical structure [16] of the alkyl chains varies from linear structure for short chains C_2-C_8, then into a loop-like structure with one coil for C_{10}-C_{16}, and into more than one coil for longer chains (≥ C18).

Table 2. Corrosion parameter for mild steel in 20% formic acid in absence and presence of the gemini surfactants from weight loss measurements at 30 ^{o}C.

Inhibitor conc. / (ppm)	Weight loss/ (mg)	Inhibition efficiency/ (%)	Corrosion rate/ (mmpy)
Blank	308.10	-	14.31
HEAB			
50	167.90	45.49	7.80
100	155.10	48.88	7.30
150	114.20	62.92	5.30
200	103.40	66.45	4.80
250	94.70	69.25	4.40
300	14.70	95.24	0.68
350	13.90	95.45	0.65
400	13.40	95.66	0.62
450	11.80	96.15	0.55
500	11.20	96.36	0.52
DDEAB			
50	155.00	49.68	7.20
100	119.00	63.66	5.20
150	92.60	69.95	4.30
200	88.30	71.34	4.10
250	13.80	96.92	0.44
300	13.40	97.14	0.40
350	8.40	97.27	0.39
400	6.00	97.98	0.28
450	5.80	98.05	0.27
500	4.70	98.96	0.22
HDEAB			
50	75.40	75.54	3.50
100	13.30	95.73	0.61
150	10.90	96.43	0.51
200	9.00	97.13	0.41
250	7.90	97.41	0.37
300	5.60	98.18	0.26
350	5.40	98.25	0.25
400	5.20	98.32	0.24
450	4.70	98.46	0.22
500	3.50	98.88	0.16

Therefore, the geometric length of the hydrophobic chains is arranged as (C_6) hexane-diyl-1,2-ethane-bis ammonium bromide (HEAB) < (C_{12}) N-dodecane-diyl-1,2-ethane-bis ammonium bromide (DDEAB) < (C_{16}) N-hexadecane-diyl-1,2-ethane-bis ammonium bromide (HDEAB). By increasing the geometric length, the isolation between metal-medium interaction increases and hence the efficiency of the corrosion inhibitor increases.

IE for compounds such as HDEAB and DDEAB doesn't show any appreciable change with increase in temperature from 30 ºC to 50 ºC (Fig. 2(b)), indicating that the inhibitive film formed on the metal surface is protective up to 50 ºC. IE of HEAB, decreases with increase in temperature, which may be due to desorption of the inhibitor from metal surface. Fig. 2(c) indicates that all

compounds attain a maximum IE at 20% formic acid and decrease on increasing the acid concentration due to increase in the aggressiveness of the acid. It is clear from Fig. 2(d), that there is no such change in IE with increase in test duration acid concentration from 24 to 96 hours, thereby suggesting that the adsorbed layer of all the compounds is effective over a long duration.

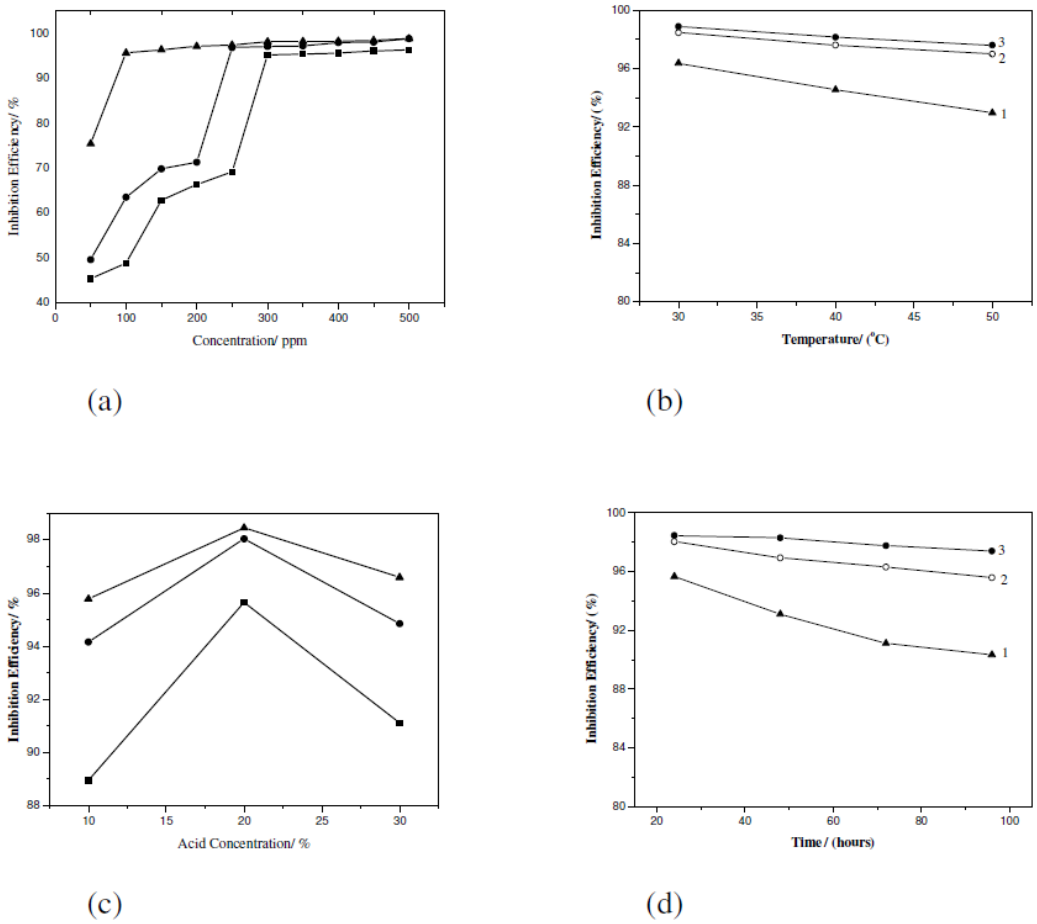

Figure 2. Variation of the inhibition efficiency with (a) inhibitor concentration; (b) temperature; (c) acid concentration; (d) immersion time of gemini surfactants in 20% formic acid (1- HEAB, 2- DDEAB, 3- HDEAB).

Application of adsorption isotherm

The mechanism of corrosion inhibition may be explained on the basis of the adsorption behaviour of the inhibitors [17]. The degree of surface coverage (θ) for different inhibitor concentrations was evaluated from weight loss measurements. It is observed that plot obeys Langmuir adsorption isotherm through surface coverage of inhibitor adsorption on mild steel surface. Langmuir isotherm is given by the following equation:

$$C_{inhi} / \theta = 1 / K_{ads} + C_{inhi} \qquad (6)$$

The plots of Cinhi / θ vs. Cinhi yielded straight lines with near unit slopes for all the gemini surfactants, showing that the adsorption model of these surfactants follows the Langmuir isotherm with good correlation (Fig. 3).

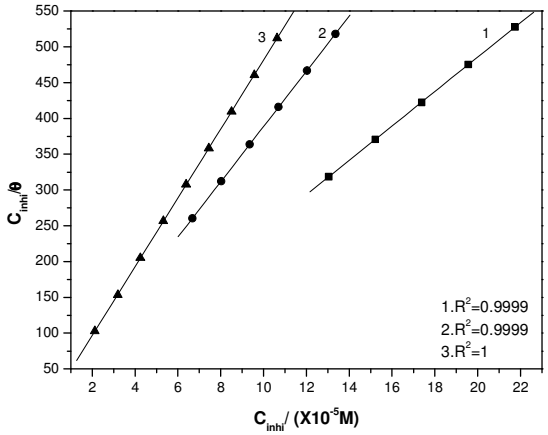

Figure 3. Langmuir adsorption isotherm plot of gemini surfactants in 20% formic acid on the surface of mild steel (1- HEAB, 2- DDEAB, 3- HDEAB).

The higher inhibitive property of gemini surfactants is attributed to the presence of quaternary nitrogen atom and the alkyl chain length which covers greater coverage of the metallic surface [18]. The values of activation energy (E_a) were calculated using the Arrhenius equation [19, 20].

$$ln\frac{r_2}{r_1} = \frac{-E_a \Delta T}{RT_1T_2} \quad (7)$$

where: r_1 and r_2 are the corrosion rates; E_a is the activation energy; T_1 and T_2 are the temperatures; $\Delta T = T_2 - T_1$; R is the gas constant.

The Gibb's free energy of adsorption (ΔG_{ads}) at different temperatures was calculated from the equation:

$$\Delta G_{ads} = - RT\, ln(55.5K) \quad (8)$$

ΔG_{ads} is the free energy of adsorption; T is the temperature in Kelvin; K is the equilibrium constant, being K given by:

$$K = \theta / C(1-\theta) \quad (9)$$

where θ is the degree of surface coverage on the metal surface; C is the inhibitor concentration.

Values of E_a and ΔG_{ads} at different temperatures are given in Table 3. E_a values for inhibited systems are higher than those of uninhibited systems, indicating that all the inhibitors are more effective at room temperature [21]. The smaller spacer and long alkyl chain, the denser will be the adsorption layer on the mild steel surface, and thus higher efficiency for inhibition of iron dissolution, which is coincident to the increment of E_a. The low and negative values of Gibb's free energy of adsorption (ΔG_{ads}) indicate spontaneous adsorption and strong interaction of the inhibitor molecule with the mild steel surface [22, 23].

Table 3. Activation energy (E_a) and Gibb's free energy of adsorption (ΔG_{ads}) for mild steel in 20% formic acid in absence and presence of gemini surfactants.

System	E_a / (KJ mol^{-1})	ΔG_{ads} / (KJ mol^{-1})		
		30 °C	40 °C	50 °C
Blank	51.28	-	-	-
HEAB	79.13	36.47	36.57	37.01
DDEAB	78.29	37.71	37.64	39.49
HDEAB	82.01	38.14	38.07	38.58

The micellization of surfactant molecules and their size and shape in aqueous media are mainly influenced by the length of the hydrophobic tails and interaction charged head groups [24]. The adsorption becomes larger as the difference in the chain length of the molecules increases. Smaller spacer size [25] means shorter distance between two head groups in unit gemini molecule and thus the charge density of the head groups is enhanced, which is further more favorable for the adsorption of the surfactant. Fig. 3 indicates that the first step occurs at very low concentration and corresponds to a binding of individual dimeric surfactants to charged sites. With further increase in the surfactant concentration in the solution, more molecules are adsorbed around initial occupied surfactants by hydrophobic interaction and finally form the surface aggregates.

Electrochemical polarization measurements

The electrochemical corrosion parameters current density (I_{corr}), corrosion potential (E_{corr}), anodic and cathodic Tafel slopes (b_a and b_c) obtained from polarization measurements are listed in Table 4. Fig. 4 shows polarization curves for mild steel in 20% formic acid without and with different gemini surfactants.

Table 4. Electrochemical polarization parameters for mild steel in 20% formic acid in absence and presence of 300 ppm concentration of different gemini surfactants.

System	E_{corr} / (mV vs. SCE)	I_{corr} / (mA cm^{-2})	b_c / ($mVdec^{-1}$)	b_c / ($mVdec^{-1}$)	IE / (%)
Blank	-417	0.320	97.7	66.0	-
HEAB	-418	0.020	116.8	50.6	93.75
DDEAB	-422	0.0095	117.0	58.6	97.03
HDEAB	-430	0.0090	135.2	64.3	97.18

The anodic and cathodic current-potential curves were extrapolated up to their interaction point. Tafel cathodic slope (b_c) suggests that the inhibiting action is a consequence of a simple blocking of the electrode by the surfactants. This way, the surface area available for hydrogen evolution is decreased, while the actual

reaction mechanism remains unaffected. The same effect was observed for the anodic slope (b_a).

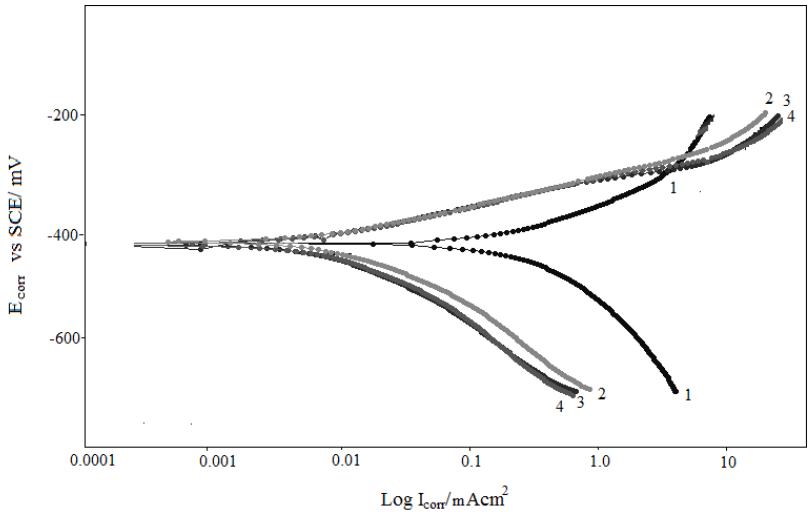

Figure 4. Potentiodynamic polarization curves for mild steel in 20% formic acid in the absence and presence of 300 ppm of different gemini surfactants (1- blank, 2- HEAB, 3- DDEAB, 4- HDEAB).

The corrosion of mild steel in formic acid solution may be considered in the following steps [3]:

$$Fe + HCOO^- \rightarrow [Fe(HCOO)]_{ads} + e^- \quad (10)$$

$$[Fe(HCOO)]_{ads} \rightarrow [Fe(HCOO)]^+ + e^- \quad (11)$$

$$[Fe(HCOO)]^+ \rightarrow Fe^{2+} + HCOOH \quad (12)$$

The evolution of hydrogen occurs as the cathodic reaction by the following mechanism:

$$Fe + HCOOH + e^- \rightarrow FeH_{ads} + HCOO^- \quad (13)$$

$$FeH_{ads} + FeH_{ads} \rightarrow H_2 + Fe \quad (14)$$

The adsorption of formate ions on the surface of iron is a precursor for the anodic dissolution and the rate of corrosion depends on the concentration of formate ion in the solution. The conductance of formic acid solution gradually increases in the concentration range from 5% - 20%. As a result, the extent of adsorption of formate ion, as well as the rate of forward step (10), increase and consequently the rate of corrosion also increases. Adsorption of inhibitor molecules on the metallic surface often involves the removal of the adsorbed water molecules, replacing them with anions from the acid and with the inhibitor. The first step of the corrosion process of mild steel in 20% formic acid solution with added inhibitor is [26]:

$$Fe + Inh \rightarrow Fe(Inh)_{ads} \quad (15)$$

$$Fe(Inh)_{ads} \rightarrow Fe^{n+} + ne^{-} + Inh \quad (16)$$

In the beginning, when concentration is low or the adsorption rate is slow, there is not enough $Fe(Inh)_{ads}$ to cover the metal surface and metal dissolution takes place on sites on the mild steel surface free of $Fe(Inh)_{ads}$. With high inhibitor concentration and especially above cmc, a compact and coherent inhibitor layer is formed on mild steel, which reduces chemical attacks on the metal. The change in E_{corr} values and decrease in the corrosion current density is observed with the addition of gemini surfactant. According to Riggs and others [27, 28], if the displacement in E_{corr} is >85 mV with respect to E_{corr}, the inhibitor can be seen as a cathodic or anodic type. In our study the maximum displacement was 15 mV, which indicates that the inhibitors are mixed-type. Maximum decrease in I_{corr} is observed for HDEAB (0.048 mA/cm^{-2}), indicating it as the most effective corrosion inhibitor among the series.

Electrochemical impedance study

Nyquist plot obtained from mild steel in 20% formic acid with the presence and absence of different gemini surfactant is shown in Fig. 5. The values of charge transfer resistance R_t, double-layer capacitance C_{dl} and IE obtained from the plot are given in Table 5.

Table 5. Electrochemical impedance parameters for mild steel in 20% formic acid in absence and presence of 300 ppm concentration of various gemini surfactants.

System	R_t / (ohmcm^2)	C_{dl} / (μFcm^{-2})	IE / (%)
Blank	75.0	118.4	-
HEAB	735.2	25.2	89.79
DDEAB	973.3	19.5	92.33
HDEAB	1032.4	13.8	93.23

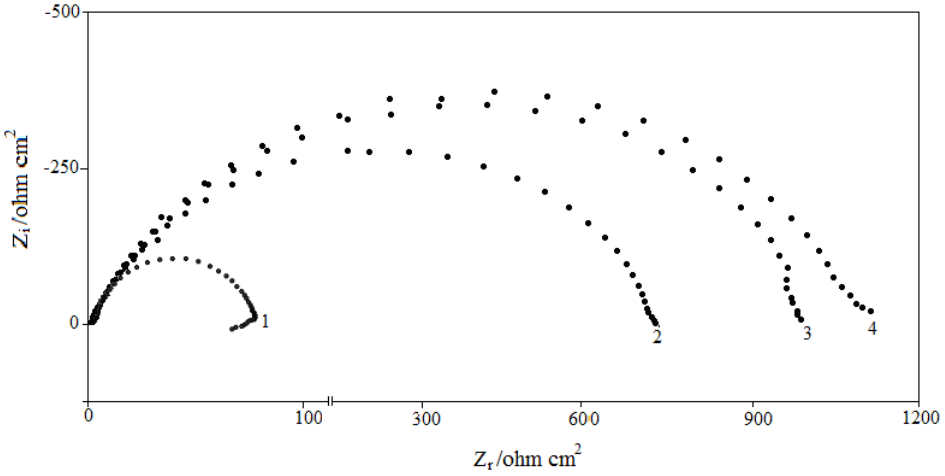

Figure 5. Nyquist plots for mild steel in 20% formic acid containing 300 ppm of different gemini surfactants (1-blank, 2- HEAB, 3- DDEAB, 4- HDEAB).

Results obtained from the impedance measurement show that R_t values increase and C_{dl} values decrease. The decrease in C_{dl} is due to increase in the thickness of the electronic double layer [29]. The increase in R_t value is attributed to the formation of a protective film on the metal/solution interface [30, 31]. These values suggest that gemini surfactants function by adsorption at the metal/solution interface, leading to a protective film on the mild steel surface [32]. The inhibition efficiency of the inhibitors is characterized by an increase in the diameter of the capacitive loop. The analysis of the parameter associated with the capacitive loop reveals that the capacity of the double layer decreases with the effectiveness of the inhibitor. This suggests that when the gemini surfactant adsorbs on the metal surface, it influences the double layer. This causes decrease in the electrical capacity and it may be attributed to the formation of a protective layer on the metal surface [25].

Scanning electron microscopy

SEM study (Fig. 6(a-c)) shows that the inhibited metal surface is found to be smoother than the uninhibited metal surface, because the inhibitor gets adsorbed on the metal surface, which shows less abrasion and corrosion on mild steel surface as compared to uninhibited metal surface.

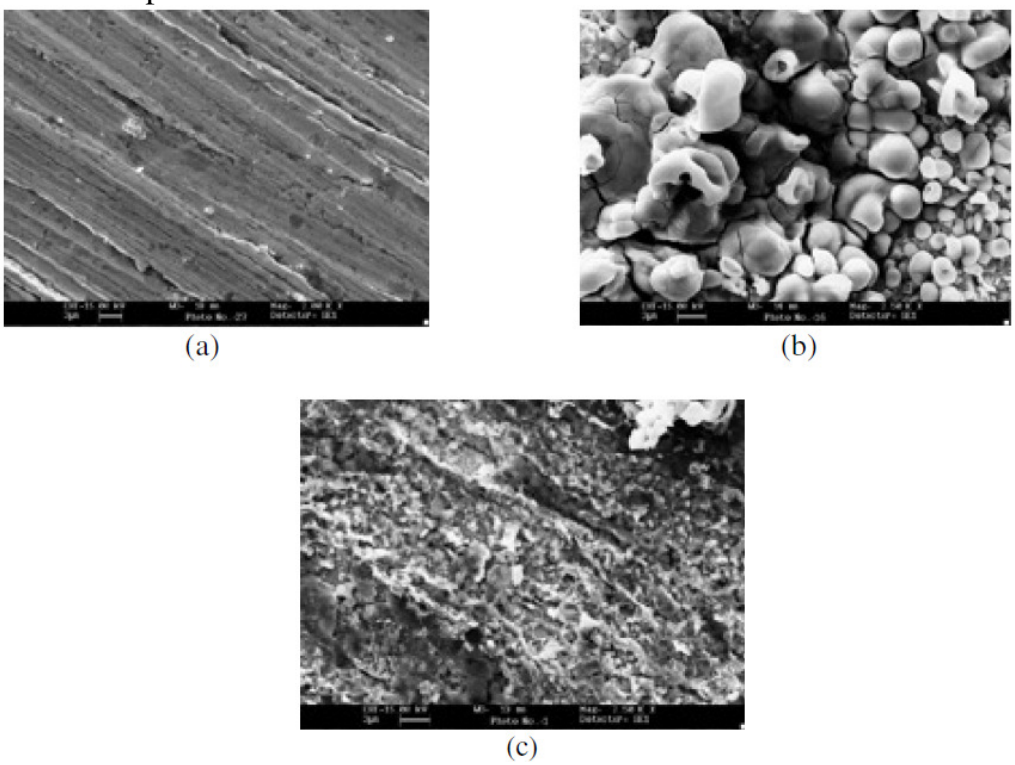

Figure 6. Mode of adsorption of gemini surfactant on mild steel surface.

Mechanism of corrosion inhibition on the basis of adsorption model

The inhibition efficiency data and the Fig. 3 show that the adsorption behaviour of gemini surfactant is more complicated than that of conventional surfactant. The adsorption of surfactant before multi layer forms three different modes of adsorption:

(1) At low concentrations, it seems that the adsorption takes place by horizontal binding of the surfactant molecule (Fig. 7(a)). This adsorption is favoured by an electrostatic interaction between the two ammonium groups (N^+) and the cathodic sites on the one hand, and on the metallic surface on the other hand.
(2) When the inhibitor concentration increases, a perpendicular adsorption takes place as a result of an inter-hydrophobic chain interaction Fig. 7(b).
(3) On further increase of the inhibitor concentration, lateral interaction increases gradually, one hydrophilic ionic group of gemini surfactant is adsorbed onto the surface, while the other hydrophilic group is free in the solution phase Fig. 7(c) and both can co-exist Fig. 7(d).
(4) With further increase in surfactant, around cmc value an efficiency plateau appears. As shown from electrochemical impedance there is one capacitive loop at high frequencies which some authors [33-35] attributed to the formation of a biomolecular layer on the metal surface Fig. 7(e).

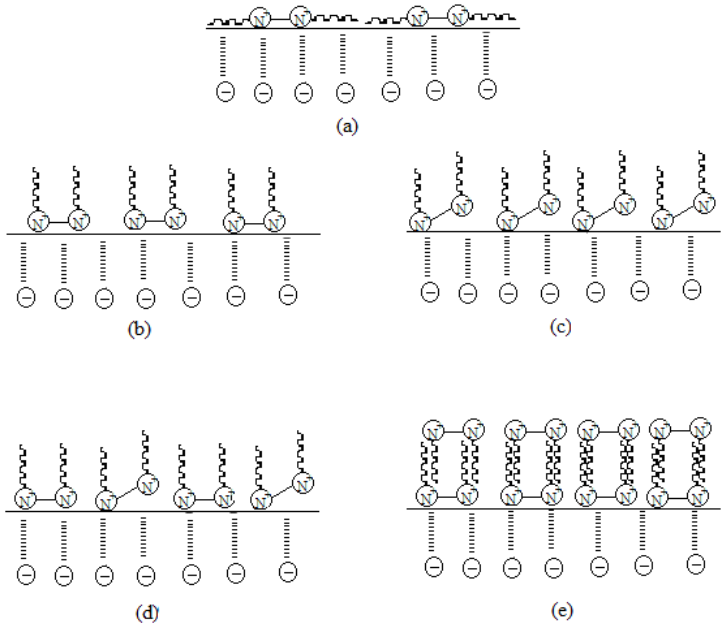

Figure 7. SEM micrographs of mild steel samples: (a) polished surface, (b) after immersion in 20% formic acid without inhibitor, (c) after immersion in 300 ppm of HDEAB.

Conclusions

(i) All the synthesized gemini surfactants showed good performance as corrosion inhibitors for mild steel. Their inhibition efficiency is concordant to their order of cmc(s).
(ii) Electrochemical studies showed that the inhibitors adsorb on the air-water interface and form a film on the metal surface.
(iii) All of the three inhibitors, inhibited corrosion by adsorption mechanism and the adsorption of these compounds follow Langmuir's adsorption isotherm.

(iv) Scanning electron microscopy shows smoother surface of inhibited metal samples than uninhibited samples due to the formation of a film on inhibited metal samples.

Acknowledgement
One of the authors F. A. Ansari, thankfully acknowledges CST UP, Lucknow, India, for the award of Young Scientist.

References

1. E. Heitz, *Corrosion of Metals in Organic Solvents*, Plenum Press, New York, NY, 1974, pp. 226.
2. V.B. Singh, R.N. Singh, *Corros. Sci.* 37 (1995) 1399. [10.1016/0010-938X(95)00042-I]
3. M.M. Singh, A. Gupta, *Mat. Chem. Phys.* 46 (1996) 15. [10.1016/0254-0584(96)80124-6]
4. L. Garverich, *Corrosion in Petrochemical Industry*, ASM International, The Materials Information Society, 1994, pp.197.
5. A. Tizpar, Z. Ghasemi, *Appl. Surf. Sci.* 252 (2006) 8630. [10.1016/j.apsusc.2005.11.084]
6. M.A. Migahed, *Mater. Chem. Phys.* 93 (2005) 48. [10.1016/j.matchemphys.2005.02.003]
7. M.A. Deyab, *Corros. Sci.* 49 (2007) 2315. [10.1016/j.corsci.2006.10.035]
8. N.A. Negm, A.S. Mohamed, *J. Surfact. Deterg. 7* (2004) 23. [10.1007/s11743-004-0284-z]
9. S.T. Kerra, N.A. Negm, S.M. Ahmed, A.M. Badwai, *J. Sci. Indus. Res.* 61 (2002) 712.
10. M. El Achouri, M.R. Infante, F. Izquierdo, S. Kertit, H.M. Gouttaya, B. Nciri, *Corros. Sci.* 43 (2001) 19. [10.1016/S0010-938X(00)00063-9]
11. F.M. Menger, C.A. Littau, *J. Am. Chem. Soc.* 115 (1993) 10083. [10.1021/ja00075a025]
12. R. Zana, *Adv. Colloid Interf. Sci.* 97 (2002) 203. [10.1016/S0001-8686(01)00069-0]
13. ASTM, *Standard Practice for Laboratory Immersion Corrosion Testing of Metals*, Annual Book of Standards, G 31-72, 3.02, 1990.
14. J. Mohan, S. Joshi, R. Prakash, R.C. Srivastava, *Electroanalysis* 167 (2004) 572. [10.1002/elan.200302841]
15. D.Q. Zhang, L.X. Gao, G.D. Zhou, *Mater. Corros.* 58 (2007) 596. [10.1002/maco.200604046]
16. N.A. Negm, S.M.I. Morsy, *J. Surfact. Deterg.* 8 (2005) 283. [10.1007/s11743-005-0359-x]
17. M.A. Quraishi, A.S. Mideen, M.A.W. Khan, M. Ajmal, *Indian J. Chem. Technol.* 1 (1994) 329.
18. L.G. Qiu, A.J. Xie, Y.H. Shen, *Mater. Chem. Phys*. 87 (2004) 237. [10.1016/j.matchemphys.2004.06.014]
19. R.T. Vashi, V.A. Champaneri, *Ind. J. Chem. Tech.* 4 (1997) 180.

20. M.A. Quraishi, F.A. Ansari, *J. Appl. Electrochem.* 36 (2006) 309. [10.1007/s10800-005-9065-z]
21. I.N. Putilova, S.A. Blazin, U.P. Baranik, *Metal Corrosion Inhibitors*, Pergamon Press, New York, NY, 1960, pp. 31.
22. Y.A. El-Awady, A.I. Ahmed, *J. Ind. Chem.* 24A (1985) 601.
23. E.E .Oguzie, V.O. Njoku, C.K. Enenbebeaku, C.O. Akalezi, C. Obi, *Corros. Sci.* 50 (2008) 3480. [10.1016/j.corsci.2008.09.017]
24. D. Asefi, M. Arami, A.A. Sarabi, N.M. Mahmoodi, *Corros. Sci.* 51 (2009) 1817. [10.1016/j.corsci.2009.05.007]
25. W. Huang, J. Zhao, *Colloids Surf. A: Physicochem. Eng. Aspects* 278 (2006) 246. [10.1016/j.colsurfa.2005.12.028]
26. V. Branzoi, F. Branzoi, M. Baibarac, *Mater. Chem. Phys.* 65 (2000) 288. [10.1016/S0254-0584(00)00260-1]
27. O.L. Riggs, *Corrosion* 31 (1975) 128.
28. E.S. Ferreira, C. Giancomelli, F.C. Giacomelli, A. Spinelli, *Mater. Chem. Phys.* 83 (2004) 129. [10.1016/j.matchemphys.2003.09.020]
29. M.G. Hosseini, M. Ehteshamzadeh, T. Shahrabi, *Electrochim Acta* 52 (2007) 3680. [10.1016/j.electacta.2006.10.041]
30. F. Bentiss, M. Traisnel, M. Lagrenee, *Corros. Sci.* 42 (2000) 127. [10.1016/0013-4686(96)00177-6]
31. S. Murlidharan, K.L.N. Phani, S. Pitchumani, S. Ravichandran, S.V.K. Iyer *J. Electrochem. Soc*. 142 (1995) 1478. [10.1149/1.2048599]
32. M. Bouklah, B. Hammouti, A. Aouniti, M. Benkaddour, A. Bouyanzer, *Appl. Surf. Sci.* 252 (2006) 6236. [10.1016/j.apsusc.2005.08.026]
33. N. Hajjaji, I. Ricco, A. Srhiri, A. Lattes, M. Soufiaoui, A.B. Bachir, *Corrosion* 49 (1993) 326.
34. W.J. Lorenz, F. Mansfeld, *Electrochim. Acta* 31 (1986) 71. [10.1016/0013-4686(86)80063-9]
35. A. Srhiri, M. Etman, F. Dabosi, *Werkst. Korros.* 43 (1992) 406. [10.1002/maco.19920430806]